NEURAL REGENERATION RESEARCH
August 2015, Volume 10, Issue 8
www.nrronline.org

RESEARCH ARTICLE

Activation of immediate-early response gene c-Fos protein in the rat paralimbic cortices after myocardial infarction

Ji Yun Ahn[1, 2, #], Hyun-Jin Tae[3, #], Jeong-Hwi Cho[4], In Hye Kim[4], Ji Hyeon Ahn[4], Joon Ha Park[4], Dong Won Kim[5], Jun Hwi Cho[2], Moo-Ho Won[4], Seongkweon Hong[6], Jae-Chul Lee[4, *], Jeong Yeol Seo[5, *]

1 Department of Emergency Medicine, Sacred Heart Hospital, College of Medicine, Hallym University, Anyang, South Korea
2 Department of Emergency Medicine, School of Medicine, Kangwon National University, Chuncheon, South Korea
3 Department of Biomedical Science and Research Institute for Bioscience and Biotechnology, Hallym University, Chunchon, South Korea
4 Department of Neurobiology, School of Medicine, Kangwon National University, Chuncheon, South Korea
5 Department of Emergency Medicine, Chuncheon Sacred Heart Hospital, College of Medicine, Hallym University, Chuncheon, South Korea
6 Department of Surgery, School of Medicine, Kangwon National University, Chuncheon, South Korea

***Correspondence to:**
Jae-Chul Lee, Ph.D. or Jeong Yeol Seo, M.D., Ph.D., anajclee@kangwon.ac.kr or siris94@hanmail.net.

 # These authors contributed equally to this work.

***doi:**10.4103/1673-5374.162757*
***http:**//www.nrronline.org/*

***Accepted:** 2015-07-04*

Abstract

c-Fos is a good biological marker for detecting the pathogenesis of central nervous system disorders. Few studies are reported on the change in myocardial infarction-induced c-Fos expression in the paralimbic regions. Thus, in this study, we investigated the changes in c-Fos expression in the rat cingulate and piriform cortices after myocardial infarction. Neuronal degeneration in cingulate and piriform cortices after myocardial infarction was detected using cresyl violet staining, NeuN immunohistochemistry and Fluoro-Jade B histofluorescence staining. c-Fos-immunoreactive cells were observed in cingulate and piriform cortices at 3 days after myocardial infarction and peaked at 7 and 14 days after myocardial infarction. But they were hardly observed at 56 days after myocardial infarction. The chronological change of c-Fos expression determined by western blot analysis was basically the same as that of c-Fos immunoreactivity. These results indicate that myocardial infarction can cause the chronological change of immediate-early response gene c-Fos protein expression, which might be associated with the neural activity induced by myocardial infarction.

***Key Words:** nerve regeneration; paralimbic cortices; myocardial infarction; c-Fos; cingulate cortex; piriform cortex; immunohistochemistry; western analysis; neural regeneration*

***Funding:** This study was supported by Hallym University Research Fund, No. 01-2012-10.*

Ahn JY, Tae HJ, Cho JH, Kim IH, Ahn JH, Park JH, Kim DW, Cho JH, Won MH, Hong S, Lee JC, Seo JY (2015) Activation of immediate-early response gene c-Fos protein in the rat paralimbic cortices after myocardial infarction. Neural Regen Res 10(8):1251-1257.

Introduction

Fos is well used as a biological marker to explore the cells that are linked to a pathogenesis induced by disorders of several organs including the central nervous system (Miwa et al., 2000; Martinez et al., 2002; Ohno et al., 2009; Wang et al., 2014; Zhu et al., 2014; Chang et al., 2015). In the brain, the selective expression of c-Fos has sometimes been observed after heart failure (Patel et al., 2000). Since the expression pattern and intensity of c-Fos differ according to conditions of brain damages, immunohistochemical detection for c-Fos has been extensively recognized as a good approach to find neuronal sub-populations in metabolically activated brain regions (Sagar et al., 1988; Hoffman et al., 1993).

Many studies showed emotional disability and depression following myocardial infarction (MI), which suggests a pathophysiological mutual relation between the heart and the brain (Frahm et al., 2004; Wann et al., 2006). Some researchers reported that neuronal damage occurred in the amygdala, a central element of the limbic system, after MI in rats (Wann et al., 2006; Kaloustian et al., 2008). The paralimbic system is an active relay structure connecting the limbic system to the neocortex, and the system is proposed as an implicated one in limbic integration including auditory-vestibular function, visceral sensory-motor function and supplement in sensorimotor function (Augustine, 1996). In addition, paralimbic regions are proposed as important structures for emotional and cognitive processing (Kalia, 2005; Izquierdo et al., 2006; Vertes, 2006; Packard, 2009).

To the best of our knowledge, the effects of MI on the paralimbic regions determined using biological markers including c-Fos have not been well understood yet. Therefore, the objective of the present study was to examine the chronological changes of c-Fos expression in the paralimbic cortices after MI in rats.

Materials and Methods

Experimental animals

Male Sprague-Dawley (SD) rats (Experimental Animal Center, Kangwon National University, Chunchon, South Korea), aged 8 weeks, weighing 280–300 g, were included in this study. These included rats were randomly assigned to a sham-operated group and six MI groups (1, 3, 7, 14, 28 and 56 days). The rats were housed in a conventional state under adequate temperature (23°C) and humidity (60%) control with a 12-hour dark-light cycle, and provided with free access to water and food. All the experimental protocols were approved by the Institutional Animal Care and Use Committee (IACUC) at Kangwon University and adhered to guidelines that are in compliance with the current international laws and policies (Guide for the Care and Use of Laboratory Animals, The National Academies Press, 8th ed., 2011).

Induction of MI

Rats were subjected to MI by a previously described method (Lee et al., 2010). Briefly, rats were intubated in a supine position and ventilated with a mixture containing 2.5% isoflurane through the use of a small animal ventilator (Model SAR-830/P, CWE Inc., Ardmore, PA, USA). Left thoracotomy was performed, and the left descending coronary artery was permanently ligated beneath the left atrial appendage with a 6-0 sterile silk. The ligation was confirmed by changing the color from red to white in the left ventricle (LV) below the ligation site and by the expansion of the left atrium just following ligating the coronary artery. Rats in the sham-operated group received the same surgical procedures with the exception of ligation of the left coronary artery. Thereafter, the rats were kept on the thermal incubator (temperature 23°C; humidity 60%) (Mirae Medical Industry, Seoul, South Korea) to maintain the body temperature of animals until they were sacrificed.

Tissue preparation for histological examination

As previously described (Lee et al., 2015), seven rats from each group were anesthetized with pentobarbital sodium (30 mg/kg, i.p.) and perfused *via* the abdominal aorta with 0.1 M phosphate-buffered saline (PBS, pH 7.4) followed by fixative solution (4% paraformaldehyde in 0.1 M phosphate-buffer (PB), pH 7.4). The hearts were harvested and embedded in paraffin blocks in each group. Sections (6 μm) of the heart were made at regular intervals of 600 μm. The brains were also harvested and post-fixed in the same fixative solution for 6 hours. The brain tissues were embedded in tissue-freezing medium and serially sectioned into 30-μm coronal sections using a cryostat (Leica, Wetzlar, Germany).

Masson's trichrome staining

The heart sections were stained to examine the result of MI using Masson's trichrome stain kit (Sigma-Aldrich, St. Louis, MO, USA) according to a method described previously (Ahmet et al., 2013). In brief, the deparaffinized sections were placed in the Biebrich scarlet-acid fuchsin and aniline blue to detect infarction area in the heart, and they were mounted in Canada balsam after the staining (Kanto chemical, Tokyo, Japan). The size of MI was calculated using a previous method (Ahmet et al., 2013) as an average percentage of endocardial and epicardial circumferences in the left ventricle that were identified as infarct area in the Masson's trichrome-stained sections.

Cresyl violet (CV) and Fluoro-Jade B (F-J B) histofluorescence staining

To elucidate the neuronal death/damage induced by MI, we performed CV and F-J B histofluorescence staining as previously described (Lee et al., 2010). In brief, the sections were stained with cresyl violet acetate solution (1.0% (w/v), Sigma-Aldrich, St. Louis, MO, USA), dehydrated in a graded ethanol series, cleared in xylene, and coverslipped. They were then mounted with Canada balsam (Kanto chemical, Tokyo, Japan). For F-J B histofluorescence, the sections were immersed in a F-J B (0.0004%, Histochem, Jefferson, AR, USA) staining solution. After washing, the sections were investigated using an epifluorescent microscope (Carl Zeiss, Göttingen, Germany) with blue (450–490 nm) excitation light and a barrier filter. F-J B-positive cells were counted in a 250 × 250 μm^2 square, selected approximately at the center of the cingulate cortex and the piriform cortex. Cell counts were obtained by averaging the total cell numbers from each rat per group.

Neuronal nuclei (NeuN) and c-Fos immunohistochemistry

The immunohistochemical staining was carried out according to a previously described method (Lee et al., 2010). The brain sections were blocked with normal goat serum (10% in 0.05 M PBS), followed by staining with primary mouse anti-NeuN (a neuron-specific soluble nuclear antigen) (diluted 1:1,000, Chemicon International, Temecula, CA, USA) and rabbit anti-c-Fos (diluted 1:200, Santa Cruz Biotechnology, Santa Cruz, CA, USA) overnight at 4°C. The sections were then incubated with mouse and rabbit secondary antibodies (room temperature, 2 hours, Vector Laboratories Inc., Burlingame, CA, USA), developed using Vectastain ABC kit (Vector Laboratories Inc.) and visualized with chromogen 3,3′-diaminibenzidine (50 mg in 100 mL of 0.1 M Tris-HCl buffer) and 0.01% hydrogen peroxidase. The negative control was performed with pre-immune serum instead of primary antibody for building up the specificity of immunostaining. The immunoreactivity of negative control was not detected in any structures. As previously described (Lee et al., 2010), the brain sections were selected according to anatomical landmarks corresponding to anterior-posterior diameter from 1.70 to −0.30 mm of rat brain atlas (Paxinos and Watson, 1986). NeuN- and c-Fos-immunoreactive cells were counted in a 250 × 250 μm^2 square selected approximately at the center of the cingulate cortex and the piriform cortex. Cell counts were obtained by averaging the total cell numbers from each rat per group.

Western blot analysis

To obtain the changes in level of c-Fos protein in the cingulate cortex and the piriform cortex after MI, as previously described (Lee et al., 2015), seven rats were sacrificed at each designated time point (3, 7, 14, 28 and 56 days) after MI and

used for western blot analysis. As previously described (Lee et al., 2014), the brain was transversely cut into sections of 400 μm thicknesses on a vibratome (Leica), and the cingulate cortex and the piriform cortex were dissected with a surgical blade under stereoscopic microscope. The tissues were homogenized in 50 mM PBS (pH 7.4) containing 0.1 mM ethylene glycol-bis (2-aminoethylether)-N,N,N′,N′-tetraacetic acid (pH 8.0), 0.2% Nonidet P-40, 10 mM ethylendiamine tetraacetic acid (EDTA) (pH 8.0), 15 mM sodium pyrophosphate, 100 mM β-glycerophosphate, 50 mM NaF, 150 mM NaCl, 2 mM sodium orthovanadate, 1 mM phenylmethylsulfonyl fluoride (PMSF) and 1 mM dithiothreitol (DTT). After centrifugation, the protein level was detected in the supernatants using a Micro BCA protein assay kit with bovine serum albumin as the standard (Pierce Chemical, Rockford, IL, USA). Aliquots containing 20 μg of total protein were boiled in loading buffer containing 150 mM Tris (pH 6.8), 3 mM DTT, 6% sodium dodecyl sulfate (SDS), 0.3% bromophenol blue and 30% glycerol. Then, each aliquot was loaded onto a 12.5% polyacryamide gel. After electrophoresis, the gels were transferred to nitrocellulose transfer membranes (Pall Crop, East Hills, NY, USA). To reduce background staining, the membranes were incubated with 5% non-fat dry milk in PBS containing 0.1% Tween 20 for 45 minutes and then with rabbit anti-c-Fos (diluted 1:1,500, 24 hours at 4°C, Santa Cruz Biotechnology), peroxidase-conjugated goat anti-rabbit IgG (diluted 1:500, 2 hours at 4°C, Sigma) and an ECL kit (Pierce Chemical, Rockford, IL, USA). Loading controls were performed using antibodies against beta-actin (Abcam Incorporated, Cambridge, MA, USA).

Statistical analysis

All data are presented as the mean ± SEM. One-way analysis of variance and a Tukey's *post hoc* test were performed to elucidate the changes of c-Fos expression between sham-operated and MI groups. Statistical analysis was performed using SAS (SAS Institute Inc., Cary, NC, USA). A level of $P < 0.05$ was considered statistically significant.

Results

Infarct size of the LV

Ligation of the left anterior descending artery could induce a distinct infarction in the anterolateral wall and apex of the LV, and the hearts showed a quickly and dynamically pathologic change after the ligation. Initially, the LV was enlarged, and subsequently a compensatory hypertrophy of myocardium was observed in non-infarcted area, and the myocardium was replaced with fibrous tissue in the infarcted area compared to the sham-operated group (**Figure 1A–F**).

In the sham-operated group, a small amount of collagen was found in the interstitial and perivascular space (**Figure 1A**). Collagen was easily observed in the infarcted wall after MI, and collagen accumulation was more increased from 3 days after MI (**Figure 1B–F**). In addition, myofibroblasts surrounding the necrotic myocardium were firstly observed in the infarcted wall from 3 days after MI. Collagen and myofibroblasts continually accumulated with time after MI, and necrotic myocardium was totally replaced with collagen and myofibroblasts in the infarcted LV at 56 days after MI (**Figure 1E–G**).

On the other hand, data of Masson's trichrome staining revealed that the infarcted region encompassed 39 – 43 % of the ventricular circumference of the LV after MI, and there was no difference in the infarct size at any time point after MI (**Figure 1H**).

Neuronal damage in the paralimbic cortices

No neurodegeneration was found in the cingulate cortex (**Figure 2A–C**) and the piriform cortex (**Figure 3A – C**) in the sham-operated group, as determined by CV staining, NeuN immunohistochemistry and F-J B histofluorescence staining. The staining pattern in the rat cingulate and piriform cortices in the MI groups was not different from that in the sham-operated group (**Figures 2D–I**, **3D–I**).

c-Fos immunoreactivity in the paralimbic cortices

c-Fos immunoreactivity was barely detected in the cingulate cortex (**Figure 4A**) and the piriform cortex in the sham-operated group (**Figure 5A**). c-Fos-immunoreactive cells in these areas were observed from 3 days after MI, continuously increased in number, peaked in the cingulate cortex at 14 days after MI and in the piriform cortex 7 days after MI; the mean number of c-Fos-immunoreactive cells was 61.8 ± 6.1/mm^2 per section from the cingulate cortex (**Figure 4B–D** and **G**) and 34.2 ± 4.4/mm^2 per section of the piriform cortex (**Figure 5B**, **C** and **G**). Thereafter, the numbers of c-Fos-immunoreactive cells in both the cingulate cortex and the piriform cortex were decreased with time after MI, and few c-Fos-immunoreactive cells were observed in both cortices at 56 days after MI (**Figure 4E–G** and **5D–G**).

c-Fos level in the paralimbic cortices

Western bolt analysis showed that the change pattern in c-Fos protein level in the cingulate and piriform cortices after MI was similar to the immunohistochemical data (**Figure 6**). c-Fos protein level in these areas was increased from 3 days and peaked at 7 and 14 days in the cingulate and piriform cortices, respectively, after MI. Thereafter, c-Fos protein levels was decreased with time after MI, and c-Fos protein level was not different from that in the sham-operated group at 56 days after MI (**Figure 6**).

Discussion

An animal model of MI can be established by blocking the blood supply of the left anterior descending artery, which may mimic human heart failure (Sun et al., 2000). Results from this study showed that there was no significant difference in the size of infarcts at any time point after MI, indicating that infarcts of similar magnitude are correlated with reduced cardiac function (Pfeffer et al., 1979; Fletcher et al., 1981).

It has been reported that MI triggers neuronal damage in the limbic regions including the hippocampus and the amygdala (Wann et al., 2006; Kaloustian et al., 2008). Findings from recent studies showed that F-J B (a high affinity

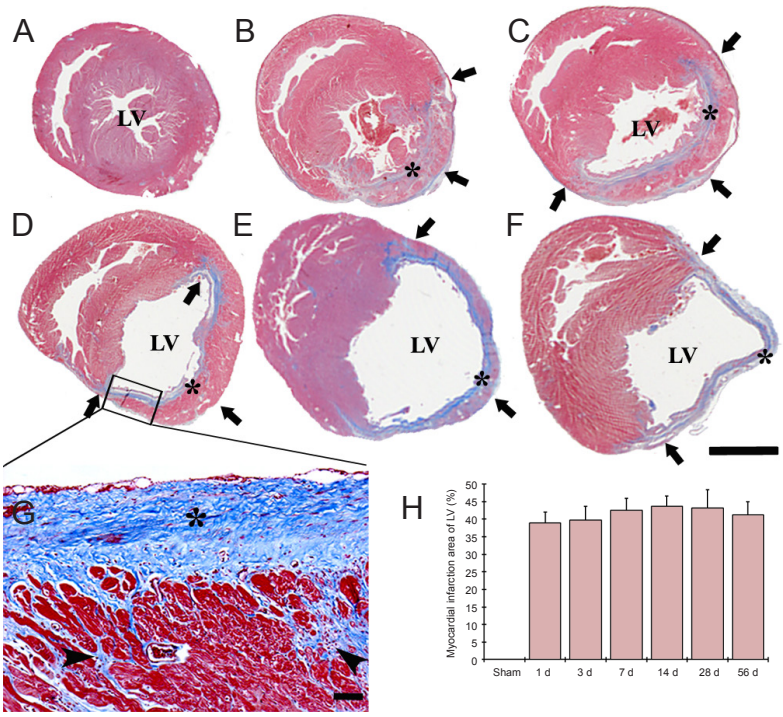

Figure 1 Masson's trichrome staining of the left ventricle (LV) wall in the sham-operated (sham) rats (A) and myocardial infarction (MI) rats at 3 (B), 7 (C), 14 (D, G), 28 (E), 56 days (F) after coronary artery ligation.

Ventricular dilation was observed in the LV after MI, the infarcted wall of the LV became thin (arrows) after MI, while the non-infarcted wall showed hypertrophy. Collagen (asterisks) was observed in the infarcted wall from 3 days after MI, and the collagen accumulated with time after MI (G). Collagen (asterisks) and myofibroblasts (arrowheads) continually accumulated after MI, and replaced by necrotic myocardium after MI (G). Scale bars: 5 mm in A–F, 50 μm in G. (H) The area of myocardial infarction in the LV ($n = 7$ rats per group). There was no significant difference in the area of myocardial infarction between each time point following MI. The bars indicate the mean ± SEM. d: Day(s).

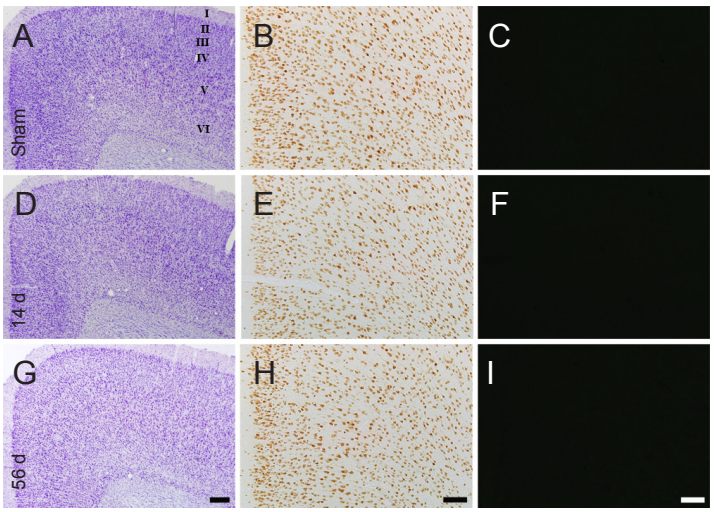

Figure 2 Cresyl violet (CV) staining (the left panels), NeuN immunohistochemistry (the middle panels) and Fluoro-Jade B (F-J B) histofluorescence staining (the right panels) of the cingulate cortex in the sham-operated rats (sham; A–C) and myocardial infarction (MI) rats at 14 (D–F) and 56 days (G–I) after MI.

In the MI groups, patterns of CV-, NeuN- and F-J B-positive cells in the cingulate cortex are similar to those in the sham group. "I–VI" indicate layers of the cingulate cortex. Scale bars: 200 μm in A, D, G and 100 μm in B, C, E, F, H and I. d: Days.

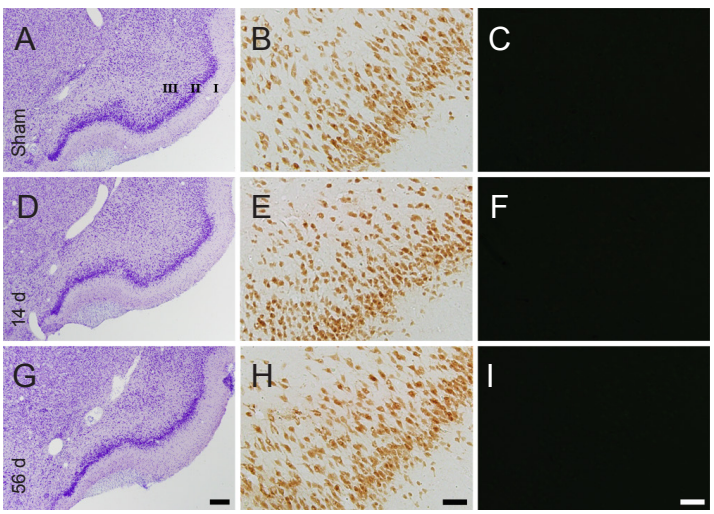

Figure 3 Cresyl violet (CV) staining (the left panels), NeuN immunohistochemistry (the middle panels) and Fluoro-Jade B (F-J B) histofluorescence staining (the right panels) of the piriform cortex in the sham-operated rats (sham; A–C) and myocardial infarction (MI) rats at 14 (D–F) and 56 days (G–I) after MI.

In the MI groups, patterns of CV-, NeuN- and F-J B-positive cells in the piriform cortex are similar to those in the sham group. "I–III" indicate layers of the cingulate cortex. Scale bars: 200 μm in A, D, G and 50 μm in B, C, E, F, H and I. d: Days.

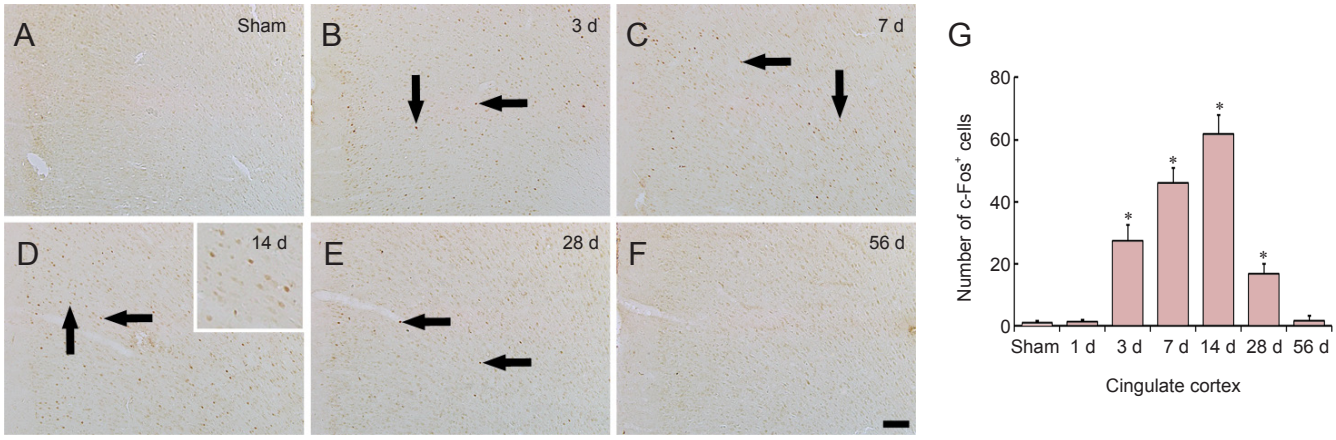

Figure 4 c-Fos immunohistochemistry in the cingulate cortex of the sham-operated (sham; A) and myocardial infarction (MI) rats at 3 (B), 7 (C), 14 (D), 28 (E) and 56 days (F) after MI.

In the sham group, c-Fos immunoreactivity was hardly detected in the cingulate cortex. In the MI groups, the number of c-Fos-positive (c-Fos$^+$) cells in the cingulate cortex (arrows) was increased at 3 d after MI, peaked at 14 d after MI, and returned to the level of the sham group at 56 d after MI. Scale bar: 100 μm. (G) The mean number of c-Fos$^+$ cells in the cingulate cortex (n = 7 rats per group); *P < 0.05, *vs.* sham group. One-way analysis of variance and a Tukey's *post hoc* test were used. The bars indicate the mean ± SEM. d: Day(s).

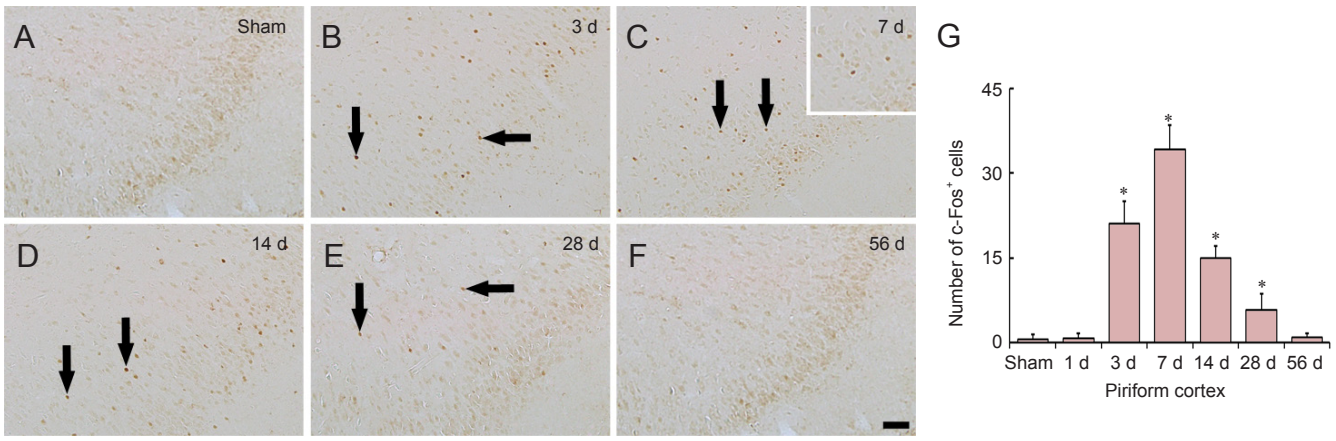

Figure 5 c-Fos immunohistochemistry in the piriform cortex of the sham-operated (sham; A) and myocardial infarction (MI) rats at 3 (B), 7 (C), 14 (D), 28 (E) and 56 days (F) after MI.

In the sham group, c-Fos immunoreactivity was hardly detected in the piriform cortex. In the MI groups, the number of c-Fos-positive (c-Fos$^+$) cells in the piriform cortex (arrows) was highest at 7 days after MI and returned to the level of the sham group at 56 d after MI. Scale bar: 100 μm. (G) The mean number of c-Fos$^+$ cells in the piriform cortex (n = 7 rats per group); *P < 0.05, *vs.* sham group. One-way analysis of variance and a Tukey's *post hoc* test were used. The bars indicate the mean ± SEM. d: Day(s).

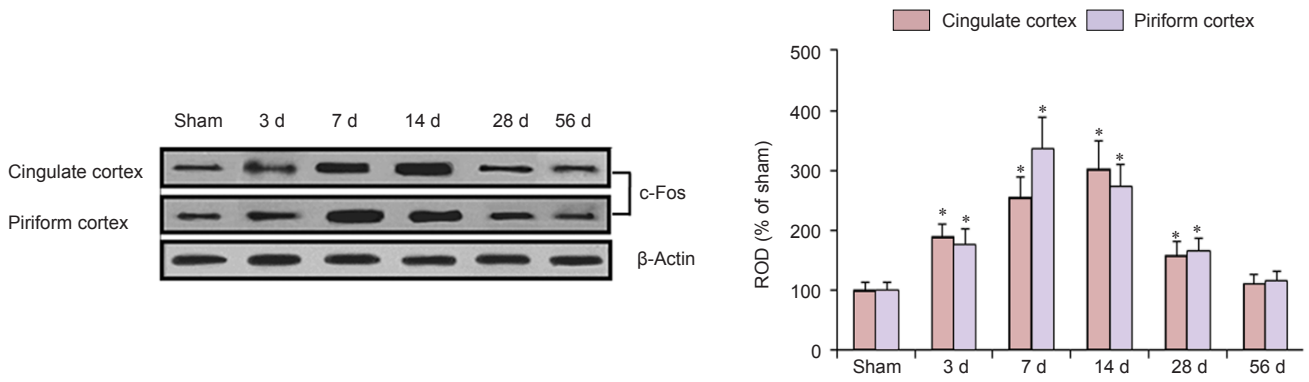

Figure 6 Western blot analysis of c-Fos protein in the cingulate and piriform cortices of the sham-operated (sham) and myocardial infarction rats at 3, 7, 14, 28 and 56 days after myocardial infarction.

The c-Fos protein expression was represented as the relative optical density (ROD) of target immunoblot band to sham band (n = 7 rats per group). *P < 0.05, *vs.* sham group; one-way analysis of variance and a Tukey's *post hoc* test were used. The bars indicate the mean ± SEM. d: Day(s).

fluorescent marker of neuronal degeneration) positive cells were found in these regions (Bae et al., 2010; Lee et al., 2010). In addition, the amygdala plays critical roles in the regulation of cardiovascular functions, feeling and cognition by regulating neuronal activity (Welch et al., 2003; Bermudez-Rattoni et al., 2004). On the basis of these results, the amygdala, which is a central part of the limbic system, is very vulnerable to MI, and patients with MI can develop dysfunction in emotion, memory and cardiovascular system.

There is increasing evidence that emotional and cognitive impairment after MI may be associated with a disproportional loss of cerebral grey matter and neuronal cells in multiple areas, such as the prefrontal cortex as a neocortex, the amygdala as a limbic cortex, and cingulate gyrus as a paralimbic cortex (Konstam et al., 2005; Rutledge et al., 2006; Drevets et al., 2008). Based on these reports, we examined neuronal damage in the paralimbic cortex and did not observe any neuronal damage in the cingulate and piriform cortices after MI using histology, NeuN immunohistochemistry and F-J B histofluorescence staining. This finding indicates that neurons in the paralimbic cortices may be less vulnerable to MI.

c-Fos has been used as a relative marker of neuronal activity in the brain after many types of brain insults (Munglani et al., 1999; Coggeshall, 2005). c-Fos incorporates with Jun to make an intracellular heterodimer that binds to activator protein-1, and it simulates further transcription of genes which are participated in many cellular cascades such as oncogenesis, apoptosis, differentiation, adjustment and remodeling (Herdegen and Waetzig, 2001; Dampney and Horiuchi, 2003).

In the central nervous system, c-Fos causes membrane depolarization and voltage-gated calcium influx, resulting in neuronal activity changes (Morgan and Curran, 1989). In addition, c-Fos is related with neuronal activation underlying learning and memory processes (Radulovic et al., 1998; Tischmeyer and Grimm, 1999). Furthermore, c-Fos has been shown to be very useful to study neuronal plasticity required for spatial memory processes (Tischmeyer and Grimm, 1999; Vann et al., 2000; Vanelzakker et al., 2011). However, a few studies have been done to examine neuronal activation in the central nervous system associated with MI (Patel et al., 2000). For examples, a study by Vahid-Ansari et al. (1998) showed a significant increase in the number of c-Fos-immunoreactive cells in the hypothalamic nuclei at 2 and 4 weeks after MI. Furthermore, in the paraventricular and supraoptic nuclei, Lindley et al. (2004) showed an augmentation of c-Fos-immunoreactive neurons at 2 and 4 weeks after MI compared to sham-operated mice. We found, in the present study, that cells in the cingulate and piriform cortices of the MI groups were immunoreactive for c-Fos from 3 days after MI, peaked in number at 7 or 14 days after MI, and were hardly observed at 56 days after MI. We also found that c-Fos levels in the cingulate and piriform cortices after MI changed in a manner similar to immunohistochemical change.

In addition, alterations in the cingulate cortex were observed in several human studies regarding anxiety disorders and/or depression (Fornito et al., 2008; Etkin et al., 2011) and inactivation in this brain region in rodents showed anxiolytic and anti-depressogenic effects (Kim et al., 2011). Anxiety disorders and/or depression are shown in the rats with MI; this symptom matches very well with the aspect of the reduced quality of life in patients with MI (Schoemaker and Smits, 1994; Schoemaker et al., 1996). The expression of c-Fos is deeply related with anxiety disorders and/or depression (Kung et al., 2010; Nestler, 2015), and anxiety and/or depression are associated with serotonin transporter dysregulation (Gross et al., 2002; Lanzenberger et al., 2010). Bielas et al. (2014) demonstrated a correlation between serotonin transporter and c-Fos expression in most brain regions affected by prenatal stress. Moreover, Iqbal Chowdhury et al. (2003) showed that cortical spreading depression affected Fos expression in the hypothalamic paraventricular nucleus and cerebral cortex of both hemispheres. Thus, we suggest that the expression of c-Fos in paralimbic cortices after MI may be related with anxiety disorders and/or depression following MI.

In conclusion, we show for the first time that MI induced neuronal damage was not observed and MI induced c-Fos expression apparently changed in the cingulate and piriform cortices. The results suggest that increased c-Fos expression in the paralimbic cortices after MI may be related with emotional and/or neurocognitive deficits associated with MI.

Acknowledgments: *We would like to thank Mr. Seung Uk Lee (Department of Physiology, College of Medicine, and Institute of Neurodegeneration and Neuroregeneration, Hallym University, Chuncheon, South Korea) for his technical help in this study.*
Author contributions: *All authors participated in the design, implementation and evaluation of the study and approved the final version of this paper.*
Conflicts of interest: *None declared.*

References

Ahmet I, Tae HJ, Brines M, Cerami A, Lakatta EG, Talan MI (2013) Chronic administration of small nonerythropoietic peptide sequence of erythropoietin effectively ameliorates the progression of postmyocardial infarction-dilated cardiomyopathy. J Pharmacol Exp Ther 345:446-456.

Augustine JR (1996) Circuitry and functional aspects of the insular lobe in primates including humans. Brain Res Brain Res Rev 22:229-244.

Bae E, Hwang IK, Yoo KY, Han TH, Lee CH, Choi JH, Yi SS, Lee SY, Ryu PD, Yoon YS, Won MH (2010) Gliosis in the amygdala following myocardial infarction in the rat. J Vet Med Sci 72:1041-1045.

Bermudez-Rattoni F, Ramirez-Lugo L, Gutierrez R, Miranda MI (2004) Molecular signals into the insular cortex and amygdala during aversive gustatory memory formation. Cell Mol Neurobiol 24:25-36.

Bielas H, Arck P, Bruenahl CA, Walitza S, Grunblatt E (2014) Prenatal stress increases the striatal and hippocampal expression of correlating c-FOS and serotonin transporters in murine offspring. Int J Dev Neurosci 38:30-35.

Chang NJ, Weng WH, Chang KH, Liu EK, Chuang CK, Luo CC, Lin CH, Wei FC, Pang ST (2015) Genome-wide gene expression profiling of ischemia-reperfusion injury in rat kidney, intestine and skeletal muscle implicate a common involvement of MAPK signaling pathway. Mol Med Rep 11:3786-3793.

Coggeshall RE (2005) Fos, nociception and the dorsal horn. Prog Neurobiol 77:299-352.

Dampney RA, Horiuchi J (2003) Functional organisation of central cardiovascular pathways: studies using c-fos gene expression. Prog Neurobiol 71:359-384.

Drevets WC, Price JL, Furey ML (2008) Brain structural and functional abnormalities in mood disorders: implications for neurocircuitry models of depression. Brain Struct Funct 213:93-118.
Etkin A, Egner T, Kalisch R (2011) Emotional processing in anterior cingulate and medial prefrontal cortex. Trends Cogn Sci 15:85-93.
Fletcher PJ, Pfeffer JM, Pfeffer MA, Braunwald E (1981) Left ventricular diastolic pressure-volume relations in rats with healed myocardial infarction. Effects on systolic function. Circ Res 49:618-626.
Fornito A, Malhi GS, Lagopoulos J, Ivanovski B, Wood SJ, Saling MM, Pantelis C, Yucel M (2008) Anatomical abnormalities of the anterior cingulate and paracingulate cortex in patients with bipolar I disorder. Psychiatry Res 162:123-132.
Frahm C, Haupt C, Witte OW (2004) GABA neurons survive focal ischemic injury. Neuroscience 127:341-346.
Gross C, Zhuang X, Stark K, Ramboz S, Oosting R, Kirby L, Santarelli L, Beck S, Hen R (2002) Serotonin1A receptor acts during development to establish normal anxiety-like behaviour in the adult. Nature 416:396-400.
Herdegen T, Waetzig V (2001) AP-1 proteins in the adult brain: facts and fiction about effectors of neuroprotection and neurodegeneration. Oncogene 20:2424-2437.
Hoffman GE, Smith MS, Verbalis JG (1993) c-Fos and related immediate early gene products as markers of activity in neuroendocrine systems. Front Neuroendocrinol 14:173-213.
Iqbal Chowdhury GM, Liu Y, Tanaka M, Fujioka T, Ishikawa A, Nakamura S (2003) Cortical spreading depression affects Fos expression in the hypothalamic paraventricular nucleus and the cerebral cortex of both hemispheres. Neurosci Res 45:149-155.
Izquierdo I, Bevilaqua LR, Rossato JI, Bonini JS, Medina JH, Cammarota M (2006) Different molecular cascades in different sites of the brain control memory consolidation. Trends Neurosci 29:496-505.
Kalia M (2005) Neurobiological basis of depression: an update. Metabolism 54:24-27.
Kaloustian S, Wann BP, Bah TM, Girard SA, Apostolakis A, Ishak S, Mathieu S, Ryvlin P, Godbout R, Rousseau G (2008) Apoptosis time course in the limbic system after myocardial infarction in the rat. Brain Res 1216:87-91.
Kim SS, Wang H, Li XY, Chen T, Mercaldo V, Descalzi G, Wu LJ, Zhuo M (2011) Neurabin in the anterior cingulate cortex regulates anxiety-like behavior in adult mice. Mol Brain 4:6.
Konstam V, Moser DK, De Jong MJ (2005) Depression and anxiety in heart failure. J Card Fail 11:455-463.
Kung JC, Chen TC, Shyu BC, Hsiao S, Huang AC (2010) Anxiety- and depressive-like responses and c-fos activity in preproenkephalin knockout mice: oversensitivity hypothesis of enkephalin deficit-induced posttraumatic stress disorder. J Biomed Sci 17:29.
Lanzenberger R, Wadsak W, Spindelegger C, Mitterhauser M, Akimova E, Mien LK, Fink M, Moser U, Savli M, Kranz GS, Hahn A, Kletter K, Kasper S (2010) Cortisol plasma levels in social anxiety disorder patients correlate with serotonin-1A receptor binding in limbic brain regions. Int J Neuropsychopharmacol 13:1129-1143.
Lee CH, Hwang IK, Choi JH, Yoo KY, Han TH, Park OK, Lee SY, Ryu PD, Won MH (2010) Calcium binding proteins immunoreactivity in the rat basolateral amygdala following myocardial infarction. Cell Mol Neurobiol 30:333-338.
Lee JC, Kim IH, Cho GS, Park JH, Ahn JH, Yan BC, Kwon HM, Kim YM, Cheon SH, Cho JH, Lee HY, Won MH, Seo JY (2014) Ischemic preconditioning-induced neuroprotection against transient cerebral ischemic damage via attenuating ubiquitin aggregation. J Neurol Sci 336:74-82.
Lee JC, Kim IH, Park JH, Ahn JH, Cho JH, Cho GS, Tae HJ, Chen BH, Yan BC, Yoo KY, Choi JH, Lee CH, Hwang IK, Kwon YG, Kim YM, Won MH (2015) Ischemic preconditioning protects hippocampal pyramidal neurons from transient ischemic injury via the attenuation of oxidative damage through upregulating heme oxygenase-1. Free Radic Biol Med 79:78-90.
Lindley TE, Doobay MF, Sharma RV, Davisson RL (2004) Superoxide is involved in the central nervous system activation and sympathoexcitation of myocardial infarction-induced heart failure. Circ Res 94:402-409.
Martinez M, Calvo-Torrent A, Herbert J (2002) Mapping brain response to social stress in rodents with c-fos expression: a review. Stress 5:3-13.
Miwa H, Nishi K, Fuwa T, Mizuno Y (2000) Differential expression of c-fos following administration of two tremorgenic agents: harmaline and oxotremorine. Neuroreport 11:2385-2390.
Morgan JI, Curran T (1989) Calcium and proto-oncogene involvement in the immediate-early response in the nervous system. Ann N Y Acad Sci 568:283-290.
Munglani R, Hudspith MJ, Fleming B, Harrisson S, Smith G, Bountra C, Elliot PJ, Birch PJ, Hunt SP (1999) Effect of pre-emptive NMDA antagonist treatment on long-term Fos expression and hyperalgesia in a model of chronic neuropathic pain. Brain Res 822:210-219.
Nestler EJ (2015) ΔFosB: a transcriptional regulator of stress and antidepressant responses. Eur J Pharmacol 753:66-72.
Ohno Y, Shimizu S, Harada Y, Morishita M, Ishihara S, Kumafuji K, Sasa M, Serikawa T (2009) Regional expression of Fos-like immunoreactivity following seizures in Noda epileptic rat (NER). Epilepsy Res 87:70-76.
Packard MG (2009) Anxiety, cognition, and habit: a multiple memory systems perspective. Brain Res 1293:121-128.
Patel KP, Zhang K, Kenney MJ, Weiss M, Mayhan WG (2000) Neuronal expression of Fos protein in the hypothalamus of rats with heart failure. Brain Res 865:27-34.
Paxinos G, Watson C (1986) The rat brain in stereotaxic coordinates, 2nd Edition. Sydney, Orlando: Academic Press.
Pfeffer MA, Pfeffer JM, Fishbein MC, Fletcher PJ, Spadaro J, Kloner RA, Braunwald E (1979) Myocardial infarct size and ventricular function in rats. Circ Res 44:503-512.
Radulovic J, Kammermeier J, Spiess J (1998) Relationship between fos production and classical fear conditioning: effects of novelty, latent inhibition, and unconditioned stimulus preexposure. J Neurosci 18:7452-7461.
Rutledge T, Reis VA, Linke SE, Greenberg BH, Mills PJ (2006) Depression in heart failure a meta-analytic review of prevalence, intervention effects, and associations with clinical outcomes. J Am Coll Cardiol 48:1527-1537.
Sagar SM, Sharp FR, Curran T (1988) Expression of c-fos protein in brain: metabolic mapping at the cellular level. Science 240:1328-1331.
Schoemaker RG, Smits JF (1994) Behavioral changes following chronic myocardial infarction in rats. Physiol Behav 56:585-589.
Schoemaker RG, Kalkman EA, Smits JF (1996) 'Quality of life' after therapy in rats with myocardial infarction: dissociation between hemodynamic and behavioral improvement. Eur J Pharmacol 298:17-25.
Sun Y, Zhang JQ, Zhang J, Lamparter S (2000) Cardiac remodeling by fibrous tissue after infarction in rats. J Lab Clin Med 135:316-323.
Tischmeyer W, Grimm R (1999) Activation of immediate early genes and memory formation. Cell Mol Life Sci 55:564-574.
Vahid-Ansari F, Leenen FH (1998) Pattern of neuronal activation in rats with CHF after myocardial infarction. Am J Physiol 275:H2140-2146.
Vanelzakker MB, Zoladz PR, Thompson VM, Park CR, Halonen JD, Spencer RL, Diamond DM (2011) Influence of pre-training predator stress on the expression of c-fos mRNA in the hippocampus, amygdala, and striatum following long-term spatial memory retrieval. Front Behav Neurosci 5:30.
Vann SD, Brown MW, Aggleton JP (2000) Fos expression in the rostral thalamic nuclei and associated cortical regions in response to different spatial memory tests. Neuroscience 101:983-991.
Vertes RP (2006) Interactions among the medial prefrontal cortex, hippocampus and midline thalamus in emotional and cognitive processing in the rat. Neuroscience 142:1-20.
Wang R, Li Z, Guo H, Shi W, Xin Y, Chang W, Huang T (2014) Caveolin 1 knockdown inhibits the proliferation, migration and invasion of human breast cancer BT474 cells. Mol Med Rep 9:1723-1728.
Wann BP, Boucher M, Kaloustian S, Nim S, Godbout R, Rousseau G (2006) Apoptosis detected in the amygdala following myocardial infarction in the rat. Biol Psychiatry 59:430-433.
Welch MG, Keune JD, Welch-Horan TB, Anwar N, Anwar M, Ruggiero DA (2003) Secretin activates visceral brain regions in the rat including areas abnormal in autism. Cell Mol Neurobiol 23:817-837.
Zhu W, Li J, Su J, Deng B, Shi Q, Zhou Y, Chen X (2014) FOS-like antigen 1 is highly expressed in human psoriasis tissues and promotes the growth of HaCaT cells in vitro. Mol Med Rep 10:2489-2494.

Copyedited by Zhang S, Zhang J, Li CH, Song LP, Zhan M